BMC Veterinary Research

RESEARCH

Open Access

Pathogenicity of tick-derived lymphocytic choriomeningitis virus in BALB/c mice

Ziyan Liu[1,2,3†], Xiaojie Liang[1†], Liang Li[3†], Ning Liu[2], Zedong Wang[2*] and Feng Wei[1*]

Abstract

Background Lymphocytic choriomeningitis virus (LCMV) is a zoonotic pathogen primarily transmitted by rodents. Recently, LCMV has been detected in ticks from northeastern China; however, the pathogenicity of this virus in murine models remains to be elucidated.

Results Here, we examined the tick-derived LCMV strain JX14 by inoculating BALB/c mice with 3.5×10^5 pfu of virus. The mice infected with LCMV displayed clinical manifestations including unkempt fur, anorexia, depression, and oliguria, which subsequently resolved by 10 days post infection (dpi) leading to survival of the infection. During the early phase of infection, low viral titers were detected in throat and anal swabs. The excreted virions demonstrated proliferation in Vero cells and were capable of inducing infection in mock-infected mice. Viral RNA was detected in the blood and organs, with detectable levels persisting for up to six months specifically in the heart. A total of 16 amino acid substitutions were identified in the L, Z, and GPC proteins between the original JX14 strain and the strain obtained after six months of infection in BALB/c mice. Pathological lesions were identified in most organs within 5 dpi except for the kidneys and testicles. Interferon gamma (IFN-γ) level was significantly elevated during the early stage of infection and returned to baseline levels within 10 days.

Conclusions This study furnishes significant insights into the pathogenic traits of the tick-derived LCMV strain JX14, thereby potentially providing a valuable in vivo research model for examining the immunological responses elicited by chronic viral infections.

Keywords Lymphocytic choriomeningitis virus (LCMV), Ticks, Pathogenicity, BALB/c mice, Rodents

Introduction

LCMV is a neglected zoonotic virus transmitted by rodents, belonging to the *Mammarenavirus* genus within the *Arenaviridae* family [1]. Infection in humans can occur through direct contact with infected rodents and their contaminated fomites, inhalation of aerosols containing the virus, transplantation of organs infected with LCMV, or congenital transmission [2]. For individuals with normal immune function, the virus typically induces mild, self-limiting, or asymptomatic infections; however, some cases may manifest as thrombocytopenia and leukopenia and progress to aseptic meningitis without long-term sequelae [3]. In contrast, immunocompromised

†Ziyan Liu, Xiaojie Liang and Liang Li contributed equally to this work.

*Correspondence:
Zedong Wang
wangzedong@jlu.edu.cn
Feng Wei
jlccwf@126.com
[1]Laboratory of Pathogen Microbiology and Immunology, College of Life Science, Jilin Agricultural University, Changchun, Jilin Province, China
[2]Department of Infectious Diseases, Center of Infectious Diseases and Pathogen Biology, Key Laboratory of Organ Regeneration and Transplantation of the Ministry of Education, State Key Laboratory of Zoonotic Diseases, The First Hospital of Jilin University, Changchun, Jilin Province, China
[3]Changchun Veterinary Research Institute, Chinese Academy of Agricultural Sciences, Changchun, Jilin Province, China

patients are at risk of developing severe systemic infection leading to mortality. Congenital infection can result in profound damage to the central nervous system and retina of fetuses, potentially causing microcephaly or even abortion [4–6].

LCMV exhibits a broad geographical distribution worldwide, including Africa, Europe, Asia, Australia, and America [7]. The common house mouse (*Mus musculus*) is the major reservoir of LCMV, which can develop a chronic, asymptomatic infection, shedding the virus via their excreta and body fluids throughout their lives. Notably, LCMV has been detected and isolated from *Ixodes ricinus* in Ukraine, as well as from at least three tick species in northeastern China [8–10]. The tick-derived LCMV strains in China exhibited distinct clades in phylogenetic trees, and demonstrated only 75.4–82.2% sequence identity with other genotype I strains at the nucleotide level [9]. These findings suggest that the tick-derived LCMV strains may possess divergent pathogenicity towards humans and mice. In this study, we established a persistent infection model in BALB/c mice using the tick-derived LCMV strain JX14, thereby facilitating the comprehensive evaluation of pathogenicity and potential transmission patterns associated with this viral strain.

Materials and methods

Virus and animals

Tick-derived LCMV strain JX14 (GenBank Accession No. MG554175 and MG554171) was used in the present study, which was isolated from *Dermacentor silvarum* ticks in 2015 in Jilin, northeastern China. The virus was propagated in African green monkey kidney cells (Vero), and stored at -80 ℃ until use. Three-week-old SPF BALB/c mice were obtained from Changsheng Biotechnology Co., Ltd. (Benxi, China). Following a one-week acclimation period in separate cages, the mice were utilized for the experiment at the Biosafety Level 3 laboratory of the Changchun Veterinary Research Institute (Changchun, China). The animal study was approved by the Animal Administration and Ethics Committee of Changchun Veterinary Research Institute of the Chinese Academy of Agricultural Sciences (Approval number: IACUC of AMMS −11-2020-026). The BALB/c mice were treated in accordance with the Animal Ethics Procedures and Guidelines of the People's Republic of China, ensuring humane handling throughout all procedures.

Animal infection and sample collection

The infection experiments were conducted based on the previous study, with necessary adjustments made based on the results of preliminary experiments [11]. Briefly, the mice were intraperitoneally inoculated with 3.5×10^5 pfu of virus, followed by a six-month monitoring period post-infection. Clinical examinations were conducted at one dpi, and lasted until 30 dpi. The mice infected with LCMV were weighed and their clinical symptoms were recorded daily. Moreover, the mice were subjected to throat and anal swab sampling, followed by suspension in 0.3 mL of Dulbecco's Modified Eagle Medium (DMEM, Gibico, USA), and subsequent storage at −80 °C until use. At each time point of 3, 5, 7, 10, 15, 30, 90, and 180 dpi, three male and three female mice were anaesthetized through inhalation of isoflurane (administered at 5%, and maintained at 2% in 100% oxygen) in order to minimize the suffering of the animals during the retroorbital blood collection. The blood samples were centrifuged at 1,000 rpm for 10 min to obtain serum. Subsequently, the animals were euthanized by cervical dislocation, and the brain, heart, lung, spleen, liver, kidney, intestine, and testicle tissues were gathered.

Virus isolation and contact transmission

All collected throat and anal swab specimens were utilized for virus isolation as previously described, employing the Vero cell line obtained from the American Type Culture Collection [9]. Briefly, 50 μL of samples were diluted 10-fold in DMEM (Gibico, USA), filtered through a syringe-driven 0.22-μm filter, and then applied onto the Vero cell monolayer for 1 h. The Vero cells in the control group were incubated with DMEM alone for the same duration. Then the cells were maintained in DMEM supplemented with 2% fetal calf serum (Sigma, Germany) at 37 °C in a 5% carbon dioxide atmosphere. After three passages, the cells were observed for cytopathic effects, and the culture supernatant was collected for LCMV RNA detection using quantitative Real-time PCR (RT-qPCR).

To determine whether the virus can be transmitted from infected mice to uninfected mice, a contact transmission experiment was conducted to assess if viral shedding is sufficient for transmission among rodents. Three male mice were intraperitoneal inoculated with 3.5×10^5 pfu of the LCMV strain JX14, and then housed in the same cage with three uninfected mice. After 15 days of co-housing, the mock-infected mice were sacrificed for the collection of brain, heart, lung, spleen, liver, kidney, and intestine tissues, and subsequently assessed for LCMV infection using RT-qPCR.

Viral RNA extraction and genome sequencing

The RNA extraction was performed on 140 μL of serum, throat swab, anal swab, and tissue homogenate supernatant specimens using a TIANamp Virus RNA Kit (TIANGEN, China). Subsequently, the extracted RNA was converted into complementary DNA utilizing a Reverse Transcription Kit (TaKaRa, Japan). Viral RNA was extracted from the hearts (at 180 dpi) of LCMV-infected mice and utilized to amplify the complete genome

sequence of the virus using the primers designed based on the tick-derived LCMV strains (Table S1).

Virus quantification assay

An RT-qPCR method was developed for the quantification of LCMV JX14 viral copy numbers (Fig. S1). Primers were designed based on the LCMV nucleocapsid protein gene, F (5′-TGATGAGTCYTTCACGTCCCA-3′), R (5′-GACAACACAGCAGCTTGACC-3′), and probe (FAM-TCACCACACCAGTTGCACCCT-BHQ1), under the following conditions: 95 °C for 30 s; followed by 50 cycles of amplification at 60 °C for 5 s and denaturation at 95 °C for 30 s. A positive result for LCMV was defined as a cycle threshold value below 40.

The plaque assay was performed as previously described [12]. In brief, after being washed twice with DMEM, Vero cells cultured in 24-well plates were inoculated with 250 μL of virus-containing supernatant that had been serially diluted tenfold, beginning with a dilution of 1:10. After incubating for 1 h at 37˚C, the inoculum was removed, and 1 mL of complete DMEM containing a 2% methylcellulose solution was added to each well. The plate was incubated for 7 days, followed by fixation with 250 μL of 4% paraformaldehyde and subsequent staining with 0.5% crystal violet for 1 h. The number of plaques per dilution was quantified and utilized to calculate the pfu/mL.

Pathological examinations and fluorescence *in situ* hybridization

Tissues comprising the spleen, lung, liver, kidney, heart, brain, intestine, and testicle from a male and a female mouse at 5 and 15 dpi, respectively, were utilized for histopathological examinations. After being preserved in formalin for 1 week and embedded in paraffin, the tissues were sectioned to a thickness of 10-μm and subsequently stained with hematoxylin and eosin.

The tissue sections were further detected for LCMV RNA distribution using fluorescence in situ hybridization (FISH), with situ hybridization probes listed in Table S2. The assay was performed according to the instructions of RNASweAMI™ RNA FISH Kit (Servicebio, China). Following the sequential steps of deparaffinization, deproteination, prehybridization, and denaturation, the tissue sections were subjected to an overnight incubation in a Cy3-labeled probe solution at a temperature of 37 °C. Subsequently, the slides underwent washing with a 1×SSC buffer (Servicebio, China) and staining with DAPI prior to mounting for subsequent immunofluorescence imaging.

Measurement of cytokine and chemokine

The levels of cytokines and chemokines in mouse sera were quantified using a Bio Plex Pro Mouse Cytokine Assay Kit (Bio-rad, USA). Ultraviolet irradiation was employed to inactivate LCMV in serum samples. Subsequently, the serum samples were tested according to the manufacturer's instructions using a Luminex 200 system. The following chemokines and cytokines were quantified using the assay: tumor necrosis factor-alpha (TNF-α), KC, IFN-γ, IL-1β, IL-2, IL-4, IL-5, IL-6, IL -10, and IL-12p70.

Statistical analysis

The figures were generated using GraphPad Prism 8 (San Diego, USA), and the statistical analyses were performed using IBM SPSS Statistics 19.0 (Chicago, USA). Statistical significance was set at $^{*}p<0.05$, $^{**}p<0.01$, $^{***}p<0.001$.

Results

Clinical signs of LCMV infection

The male and female mice infected with the LCMV strain JX14 exhibited weight loss starting from 7 to 3 dpi, respectively, and subsequently regained their original body weight at 18 and 14 dpi, correspondingly (Fig. 1A). Male mice exhibited significantly greater weight loss compared to mock-infected mice between 4 and 26 dpi, while female mice demonstrated significantly greater weight loss than mock-infected counterparts between 2 and 28 dpi. Significant weight loss was also observed in LCMV-infected male mice compared to female mice prior to 10 dpi. At 6 dpi, the subjects exhibited signs of unkempt fur, anorexia, and depression, which subsequently resolved by 10 dpi. Oliguria was observed from one dpi and returned to normal levels at 15 dpi. No mortality was recorded among the mice infected with LCMV.

LCMV viral RNA detection in mice excreta

After LCMV infection, throat and anal swabs were collected every day across the first month to evaluate viral titer. LCMV was detected in the anal swabs of both male and female mice at 4 dpi, persisting until 8 dpi, with significantly higher viral titers observed in male mice compared to female mice between 5 and 8 dpi. Additionally, the virus was detectable in the throat swabs of BALB/c mice at 4 dpi, persisting until 8 and 10 dpi in female and male mice, respectively, with significantly higher viral titers noted in male mice between 7 and 10 dpi (Fig. 1B).

Moreover, LCMV was successfully isolated from all the qPCR-positive swabs using Vero cells, and cytopathic effects were observed upon the third passage, which were subsequently confirmed by RT-qPCR (Fig. S2A, 2B). Notably, our contact transmission experiment demonstrated that among the three mock-infected mice, one tested positive for LCMV in the brain, heart, spleen, liver, and kidney; another was only positive in the kidney, while no tissues from the third mouse were found to be positive. The results indicate that, although the viral loads in

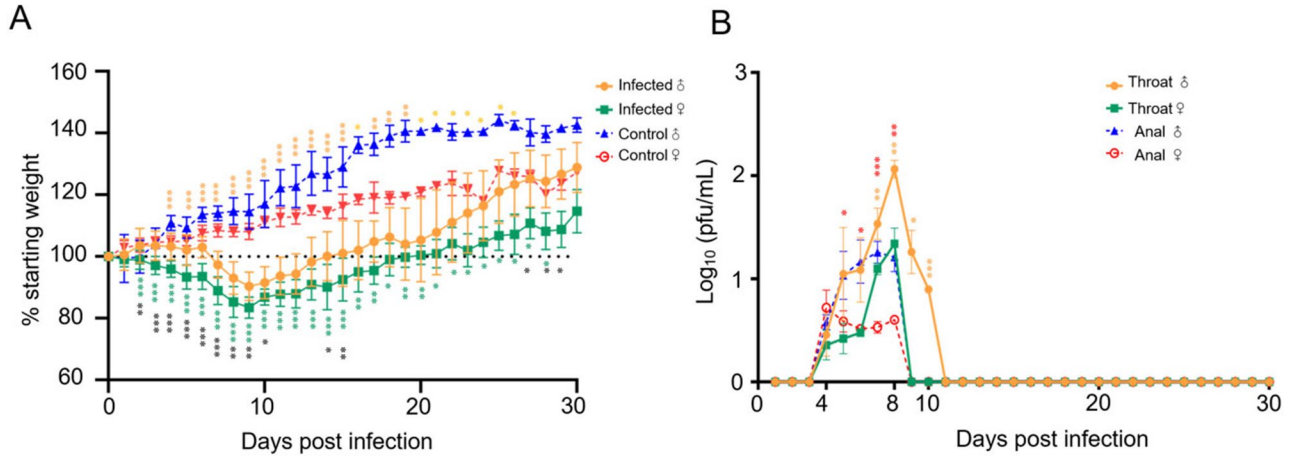

Fig. 1 Weight changes and viral excretion of lymphocytic choriomeningitis virus (LCMV) strain JX14 infected BALB/c mice. Four-week-old wild-type male ($n=3$) and female ($n=3$) BALB/c mice were inoculated intraperitoneally with 3.5×10^5 pfu of LCMV and monitored for clinical signs and viral excretion for 30 days. Same number of male and female mice were inoculated intraperitoneally with DMEM. Values are the means (±standard deviation) from two experiments. (**A**) Weight changes of LCMV infected mice. Weight change is analyzed by t-test. Black dashed line indicates 100% starting weight for reference. The p-values comparing female LCMV-infected mice to mock-infected controls are denoted by green asterisks, while those for male mice are represented by orange asterisks. Black asterisks indicate the differences between LCMV-infected male and female mice. (**B**) Virus titers (pfu/mL) quantified in the throat and anal swabs of mice. Virus titer is analyzed by t-test. The p-values comparing female to male anal swabs are denoted by red asterisks, while those for throats are represented by orange asterisks. Significance levels are defined as follows: $*p<0.05$, $**p<0.01$, $***p<0.001$

the throat and anal swabs of the infected mice were low, transmission among rodents occurred, albeit limited (Fig. S2C).

LCMV RNA load in mice tissues

To investigate the pathogenesis of the virus, male and female BALB/c mice were sacrificed at 3, 5, 7, 10, 15, 30, 90, and 180 dpi, respectively. Subsequently, viral RNA load in mouse tissues was assessed using RT-qPCR. Viral RNA was detected in all major organs, including the heart, liver, spleen, lung, kidney, brain, intestine, and testis of mice (Fig. 2A). Although viremia lasts for 15 days in all the mice, the LCMV RNA was not detectable on 10 dpi in the brain of both the male and female mice, and the brains showed the lowest LCMV RNA levels compared with other organs (Fig. 2B). In contrast to the brains, viral RNA was consistently detectable in the hearts of male mice and in both the hearts and kidneys of female mice throughout the infection, which can persist for up to 6 months (Fig. 2). Overall, the viral RNA levels in all the organs of mice reached their peaks at 3 dpi and gradually decreased as the duration of infection extended from 7 days to 6 months. Moreover, the duration and RNA load of LCMV in all organs showed prolonged persistence or sustained elevation in male mice compared with female mice. (Fig. 2). Notably, no significant difference in viral titers was observed between male and female organs during the acute phase of infection.

Pathological lesions in LCMV-infected mice

The tissue samples were collected from LCMV-infected mice at 5 and 15 dpi for the assessment of pathological lesions. At 5 dpi, pathological lesions were identified in most of the organs except in kidneys and testicles. Moderate neutrophil infiltration was observed in the hearts and livers, and scattered neutrophil infiltration was present in the spleens, lungs, and intestines (Fig. 3, Fig. S3, Table S3). Of these tissues, pathological changes within the spleen were maximal on 5 dpi, and nearly recovered on 15 dpi (Fig. 3A, Table S3). The red pulp of the spleens in LCMV-infected mice exhibited a visually reduced lymphocyte cellularity, while a significant elevation in the number of megakaryocytes was observed, suggesting the extramedullary hematopoiesis in spleen induced by LCMV (Fig. 3A). Fluorescence in situ hybridization revealed the widespread distribution of LCMV in the spleens, with a reduction observed on 15 dpi (Fig. 3B).

Cytokine and chemokine induced by LCMV infection

To establish cytokine production induced by LCMV infection in mice, serum samples collected on 3, 5, 7, 10, 15, 20, and 30 dpi were analyzed between control and LCMV infected mice. LCMV infection induced the production of inflammatory cytokines and chemokines, including IFN-γ, IL-5, IL-6, and KC (CXCL1). The expression of IFN-γ, the most upregulated cytokine in LCMV-infected mice, exhibited a significant increase from 3 dpi onwards and reached its peak at 5 dpi. Subsequently, there was a rapid decline observed at 7 dpi in both male and female mice. The level of IL-5, IL-6, and KC peaked

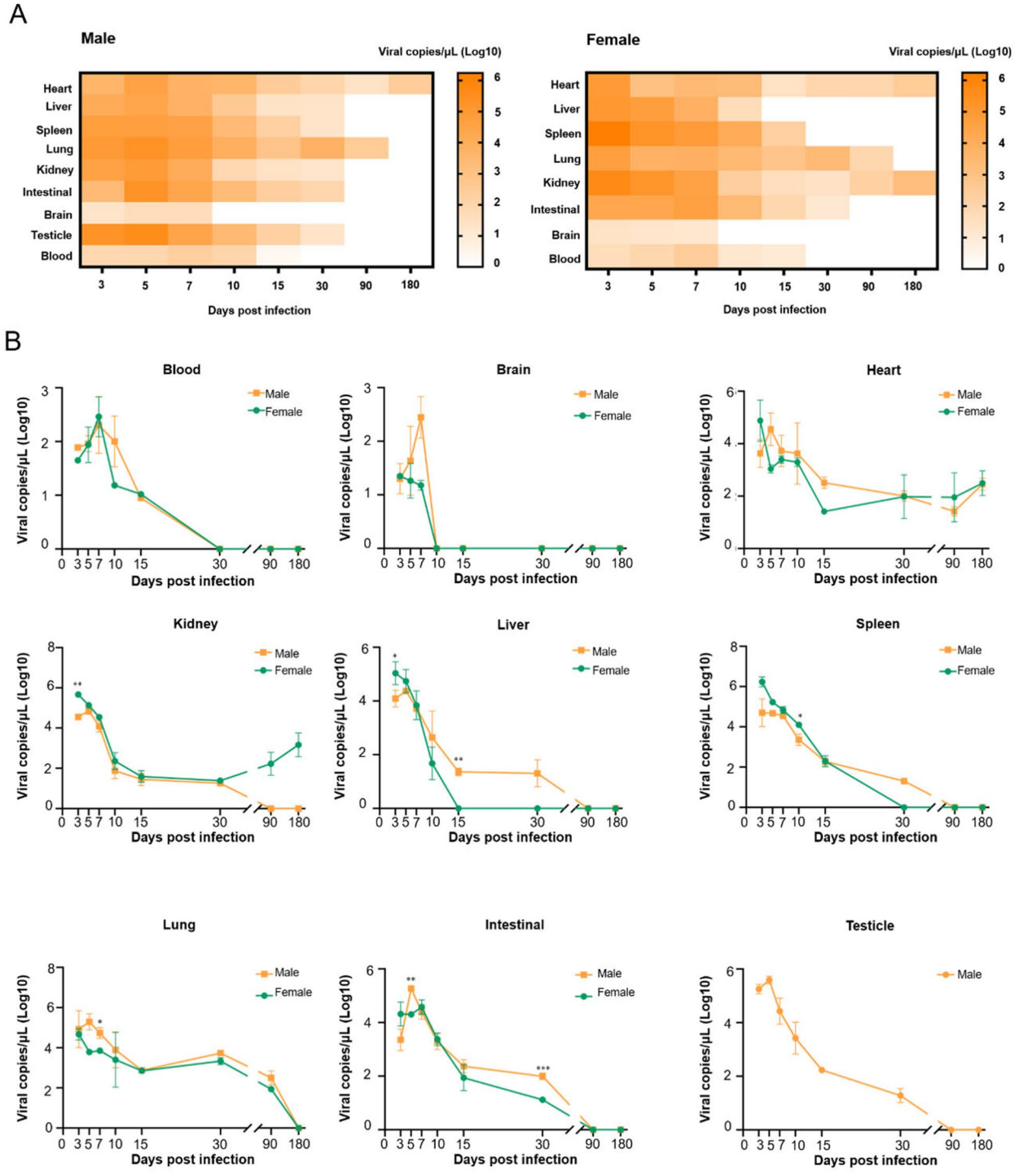

Fig. 2 Lymphocytic choriomeningitis virus (LCMV) strain JX14 RNA load in blood and tissues of BALB/c mice.Four-week-old wild-type male ($n=24$) and female ($n=24$) BALB/c mice were inoculated intraperitoneally with 3.5×10^5 pfu of LCMV and sacrificed at 3, 5, 7, 10, 15, 30, 90, and 180 dpi for tissue collection. Same number of male and female mice were inoculated intraperitoneally with DMEM. Values are the means (±standard deviation) from two experiments. (**A**) Heat maps of LCMV RNA load (copies/μL) in mice blood and tissues. (**B**) LCMV RNA load (copies/μL) in blood and different tissues of infected mice. Statistical comparison between male and female mice was conducted using t-test. Significance levels are defined as follows: $^*p<0.05$, $^{**}p<0.01$, $^{***}p<0.001$

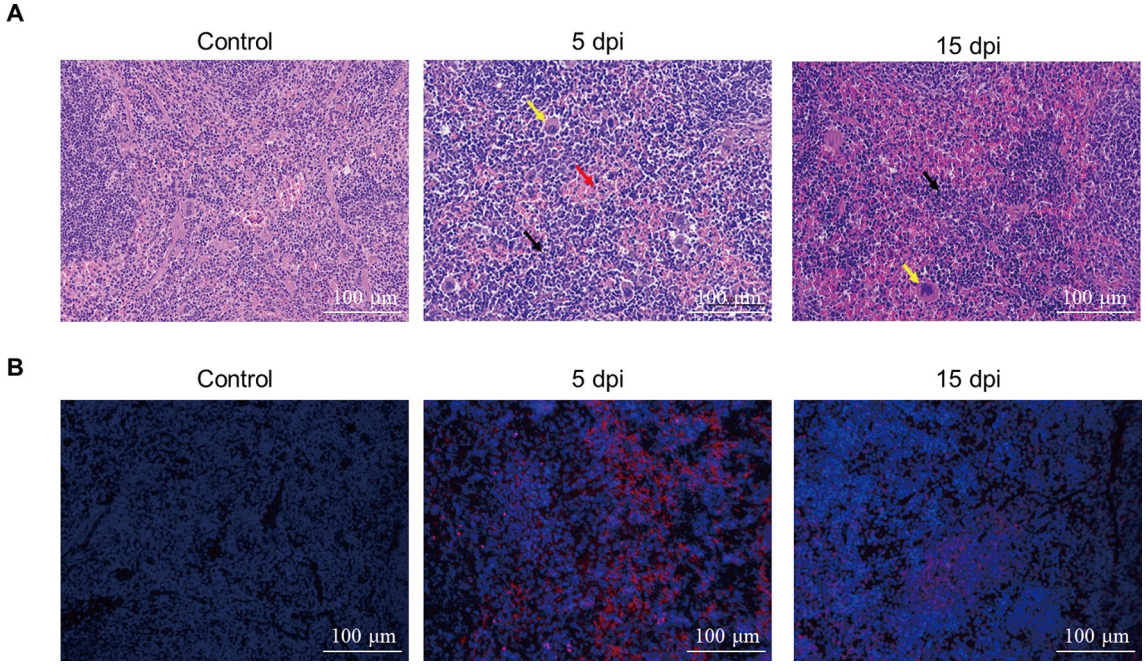

Fig. 3 Lymphocytic choriomeningitis virus (LCMV) strain JX14 causes prominent pathology in the spleens of BALB/c mice. Four-week-old wild-type male ($n=4$) BALB/c mice inoculated intraperitoneally with 3.5×10^5 pfu of LCMV were sacrificed at 5 and 15 dpi for pathology observation. Same number of female mice were inoculated intraperitoneally with DMEM. (**A**) HE staining of the spleens of LCMV-infected and mock-infected mice. (**B**) Fluorescence in situ hybridization detection of the spleens of LCMV-infected and mock-infected mice. Extramedullary hematopoietic lesions in the red pulp are indicated with black arrows, multinucleated giant cells are marked with yellow arrows, and infiltration of neutrophils are labeled with red arrows. Dpi, days post infection

at 5 dpi, and reduced at 7 dpi (Fig. 4). Overall, most of the cytokines produced by LCMV-infected mice did not exhibit significant differences and returned to baseline levels within a short timeframe (within 10 days) (Fig. S4).

Discussion

The present study aimed to evaluate the clinical manifestations, lethality, and viral RNA load in tissues of LCMV strain JX14 isolated from ticks in northeastern China using BALB/c mice. Rodents, as the natural reservoir of LCMV, can shed LCMV via excrement, urine, and saliva [1]. In this study, viral shedding kinetics in anal and throat were detected in all BALB/c mice between 4 and 8 dpi. Although viral loads in the anal and throat swabs of the infected mice were very low, our contact transmission experiment revealed the transmission among rodents, albeit limited (Fig. S2A, S2B). The findings suggest that this LCMV strain can be transmitted through mice droppings and saliva during the acute infection phase, potentially contributing to virus transmission among rodents in natural epidemic foci and increasing the risk of human LCMV infection.

It has been demonstrated that the classic LCMV strains can establish long-term non-cytolytic infection in cells and spread in culture through cell-to-cell contacts [13]. Nonetheless, the tick-derived LCMV strain is capable of inducing cytopathic effects in Vero cells, although these effects are relatively mild. The low nucleotide sequence identities (82.1–86.0% for the S segment, and 75.4–82.2% for the L segment) between our viral strain and other classic LCMV strains may contribute to the observed differences. Notably, our findings indicate that after 180 days of continuous infection in mice, the tick-derived LCMV exhibited differences from the primary strain at up to 16 amino acid sites (Table S4), suggesting a robust evolutionary capacity for this virus and contributing to our understanding of the molecular mechanisms underlying persistence in this viral strain.

To date, over 30 strains of LCMV have been identified in humans and rodents, with the viral strains classified into acute and chronic groups based on their virology and pathogenicity [7]. Of these viral strains, Armstrong 53b and WE isolated from infected patients in the 1930s, are highly pathogenic and can cause acute infection [14, 15]. Strain Clone 13, derived from the Armstrong 53b strain, exhibited a difference of only two amino acids compared to its parental strain. Nevertheless, Clone 13 was considered as the representative chronic strain that can cause persistent infection for up to 90 days [7, 16, 17]. Another LCMV strain (BRC), discovered in Japan, has been found to have low or non-pathogenic effects in mice. This strain demonstrated no clinical signs or lethality in dBa/1 mice and maintained high levels of viral genome load in the lungs of C57BL/6 mice even up to 112 dpi [11]. In this study, although severe symptoms (anorexia, emaciation, and depression) occurred in the strain JX14 infected

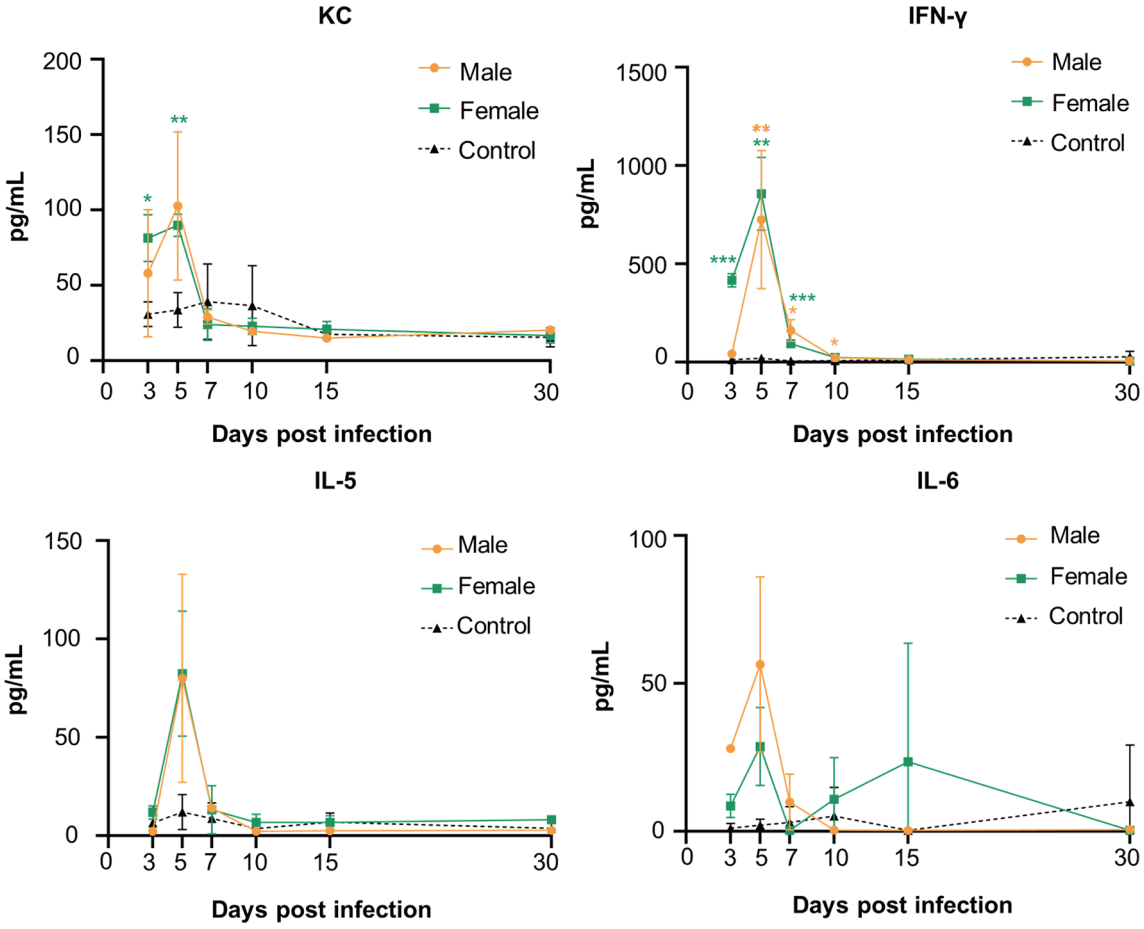

Fig. 4 Pro-inflammatory immune responses induced by lymphocytic choriomeningitis virus (LCMV) strain JX14 in BALB/c mice. Four-week-old wild-type male ($n = 18$) and female ($n = 18$) BALB/c mice were inoculated intraperitoneally with 3.5×10^5 pfu of LCMV and sacrificed at 3, 5, 7, 10, 15, 30 dpi for serum collection. Same number of male and female mice were inoculated intraperitoneally with DMEM. Values are the means (± standard deviation) from two experiments. Serum samples from the male and female infected mice or control mice are analyzed for cytokines and chemokines. Statistical comparison between male and female mice is conducted using t-test. The p-values comparing female LCMV-infected mice to mock-infected controls are denoted by green asterisks, while those for male mice are represented by orange asterisks. Significance levels are defined as follows: $^*p < 0.05$, $^{**}p < 0.01$, $^{***}p < 0.001$

mice, no one died, and our viral strain can maintain persistent nonlethal infection in BALB/c mice. High levels of viral RNA can be detected for up to 180 dpi in the hearts of male mice, and in both hearts and kidneys of female mice (Fig. 2). Notably, the viral load in BALB/c mice infected with JX14 was found to be high in the lungs and low in other tissues at 30 dpi, which exhibited a similar tissue tropism as observed for BRC and OQ28 strains but differed from that of Clone13, thereby emphasizing the shared tissue preference between JX14 and Japan strains (BRC and OQ28) [11, 16].

Cytokines are critical mediators of innate antiviral immune responses. Dysregulation of the immune responses often results in excessive production of pro-inflammatory cytokines, leading to the onset of cytokine storm, which has been confirmed in LCMV infected perforin-deficient (Prf1−/−) mice [18–20]. In this study, the tick-derived LCMV did not provoke a cytokine storm syndrome in BALB/c mice. With the exception of IFN-γ and CK, no other cytokines demonstrated significant differences between the infected and control groups. IFN-γ plays a crucial role in the pathophysiology of LCMV-infected mice, and modulation of IFN-γ expression in mice can effectively ameliorate the disease and significantly extend survival [19, 20]. As the most upregulated cytokine in our mice model, although IFN-γ peaked at 5 dpi, rapidly declined to baseline levels at 10 dpi in both male and female mice. This timepoint aligns with the resolution of clinical signs, suggesting that the mitigation of LCMV infection in mice may be associated with the rapid decrease in IFN-γ levels. Following the acute infection phase, no significant increase in related cytokines was observed, which may be one of the critical factors enabling the virus to maintain long-term infection in mice.

The LCMV mouse model serves as an indispensable in vivo research tool in the field of immunology, making significant contributions to the comprehension of

fundamental principles pertaining to both innate and specific immunity [21, 22]. For instance, the involvement of PD-1 in modulating T-cell responses to persistent viral infections was initially elucidated by employing LCMV infection in mice [23]. In this study, we established a non-lethal mouse model of chronic infection using JX14, thereby potentially providing valuable insights into the fundamental principles underlying both innate and specific immunity elicited during persistent viral infections.

There are certain limitations in this study. Firstly, it has been established by previous studies that the clinical signs, lethality, and virus distribution in mice can be influenced by factors such as mouse strain and route of inoculation. However, in our study, we only used one mouse strain (BALB/c) and administered the virus through one route (intraperitoneal injection), which may potentially introduce bias into the interpretation of our findings. In addition, considering the Animal Ethics Procedures and Guidelines about the minimizing use of laboratory animals, a limited number of male and female mice were used, which may also affect the drawing of significant sex-based conclusions. Lastly, the absence of comparator groups for several classic LCMV strains, such as Armstrong 53b, WE, and BRC, in our study precludes a comparative analysis between this tick-derived LCMV and these classical strains under our experimental conditions. This limitation hinders the objective interpretation of pathogenic differences between tick-derived LCMV and other traditional LCMV strains.

Conclusion

In summary, our study provides significant insights into the pathogenic characteristics of tick-derived LCMV strain JX14 identified in China. Although the viral infection was found to be nonlethal in both male and female BALB/c mice, persistent infection was observed in hearts and kidneys for up to six months. Considering that the mouse strain and inoculation route can influence clinical manifestations, virus distribution, and lethality of LCMV infection in mice, further investigation involving experimental infections on other mouse strains is recommended to comprehensively evaluate the pathogenic characteristics of this viral strain.

Abbreviations

DMEM	Dulbecco's Modified Eagle's medium
Dpi	days post infection
FISH	fluorescence in situ hybridization
IL	Interleukin
IFN-γ	Interferon gamma
KC	CXCL1
LCMV	Lymphocytic choriomeningitis virus
RT-qPCR	Quantitative Real-time PCR
TNF-α	Tumor necrosis factor-alpha
Vero	African green monkey kidney cells

Supplementary Information

The online version contains supplementary material available at https://doi.org/10.1186/s12917-024-04451-8.

Supplementary Material 1

Supplementary Material 2

Supplementary Material 3

Supplementary Material 4

Supplementary Material 5

Supplementary Material 6

Supplementary Material 7

Supplementary Material 8

Acknowledgements

No applicable.

Author contributions

ZW and FW conceived the study. ZL, LX, and LL performed analysis. NL provided assistance in data analysis. ZW and ZL wrote the manuscript. ZW and FW revised the manuscript. All authors read and approved the final manuscript.

Funding

This study was supported by the National Natural Science Foundation of China (32072887 and 82272327), the National Key Research and Development Program of China (2022YFC2601900), and the Bethune Project of Jilin University (2022B01).

Data availability

The complete genome sequence of the strain JX14 following 180 days of infection in BALB/c mice (JX14 180dpi) has been uploaded to GenBank, with the accession numbers PQ497238 for the L segment and PQ497239 for the S segment. The datasets generated and/or analyzed during the current study are available from the corresponding author upon reasonable request.

Declarations

Ethics approval and consent to participate

The animal study was approved by the Animal Administration and Ethics Committee of Changchun Veterinary Research Institute of the Chinese Academy of Agricultural Sciences (Approval number: IACUC of AMMS – 11-2020-026). The BALB/c mice were treated in accordance with the Animal Ethics Procedures and Guidelines of the People's Republic of China, ensuring humane handling throughout all procedures.

Consent for publication

Not applicable.

Competing interests

The authors declare no competing interests.

Received: 31 July 2024 / Accepted: 17 December 2024
Published online: 06 January 2025

References

1. Laposova K, Pastorekova S, Tomaskova J. Lymphocytic choriomeningitis virus: invisible but not innocent. Acta Virol. 2013;57(2):160–70.
2. Bonthius DJ. Lymphocytic choriomeningitis virus: an underrecognized cause of neurologic disease in the fetus, child, and adult. Semin Pediatr Neurol. 2012;19(3):89–95.
3. Pencole L, Sibiude J, Weingertner AS, Mandelbrot L, Vauloup-Fellous C, Picone O. Congenital lymphocytic choriomeningitis virus: a review. Prenat Diagn. 2022;42(8):1059–69.

4. Ferenc T, Vujica M, Mrzljak A, Vilibic-Cavlek T. Lymphocytic choriomeningitis virus: an under-recognized congenital teratogen. World J Clin Cases. 2022;10(25):8922–31.
5. Delaine M, Weingertner AS, Nougairede A, Lepiller Q, Fafi-Kremer S, Favre R, Charrel R. Microcephaly caused by lymphocytic choriomeningitis virus. Emerg Infect Dis. 2017;23(9):1548–50.
6. Ansari N, Demmler-Harrison G, Coats DK, Paysse EA. Severe congenital chorioretinitis caused by congenital lymphocytic choriomeningitis virus infection. Am J Ophthalmol Case Rep. 2021;22:101094.
7. Vilibic-Cavlek T, Savic V, Ferenc T, Mrzljak A, Barbic L, Bogdanic M, Stevanovic V, Tabain I, Ferencak I, Zidovec-Lepej S. Lymphocytic choriomeningitis-emerging trends of a neglected virus: a narrative review. Trop Med Infect Dis 2021, 6(2).
8. Hladkii AP. Study of the strain of lymphocytic choriomeningitis virus isolated from IX. ricinus ticks gathered in the western regions of the Ukrainian SSR. Mikrobiol Zh. 1965;27(1):10–5.
9. Zhang L, Li S, Huang SJ, Wang ZD, Wei F, Feng XM, Jiang DX, Liu Q. Isolation and genomic characterization of lymphocytic choriomeningitis virus in ticks from northeastern China. Transbound Emerg Dis. 2018;65(6):1733–9.
10. Liu Z, Li L, Wang D, Zhang L, Liang X, Wang Z, Wei F. Molecular detection and phylogenetic analysis of lymphocytic choriomeningitis virus in ticks in Jilin Province, northeastern China. J Vet Med Sci. 2023;85(3):393–8.
11. Takagi T, Ohsawa M, Yamanaka H, Matsuda N, Sato H, Ohsawa K. Difference of two new LCMV strains in lethality and viral genome load in tissues. Exp Anim. 2017;66(3):199–208.
12. Bricker TL, Shafiuddin M, Gounder AP, Janowski AB, Zhao G, Williams GD, Jagger BW, Diamond MS, Bailey T, Kwon JH, et al. Therapeutic efficacy of favipiravir against Bourbon virus in mice. PLoS Pathog. 2019;15(6):e1007790.
13. Labudová M, Čiampor F, Pastoreková S, Pastorek J. Cell-to-cell transmission of lymphocytic choriomeningitis virus MX strain during persistent infection and its influence on cell migration. Acta Virol. 2018;62(4):424–34.
14. Rivers TM, McNair Scott TF. Meningitis in man caused by a filterable virus. Science. 1935;81(2105):439–40.
15. Armstrong AR, King EJ, Harris RI. Phosphatase in obstructive jaundice. Can Med Assoc J. 1934;31(1):14–20.
16. Blackburn SD, Crawford A, Shin H, Polley A, Freeman GJ, Wherry EJ. Tissue-specific differences in PD-1 and PD-L1 expression during chronic viral infection: implications for CD8 T-cell exhaustion. J Virol. 2010;84(4):2078–89.
17. Oldstone MBA, Ware BC, Horton LE, Welch MJ, Aiolfi R, Zarpellon A, Ruggeri ZM, Sullivan BM. Lymphocytic choriomeningitis virus clone 13 infection causes either persistence or acute death dependent on IFN-1, cytotoxic T lymphocytes (CTLs), and host genetics. Proc Natl Acad Sci U S A. 2018;115(33):E7814–23.
18. Albeituni S, Oak N, Tillman HS, Stroh A, Keenan C, Bloom M, Nichols KE. Cellular and transcriptional impacts of Janus kinase and/or IFN-gamma inhibition in a mouse model of primary hemophagocytic lymphohistiocytosis. Front Immunol. 2023;14:1137037.
19. Binder D, van den Broek MF, Kagi D, Bluethmann H, Fehr J, Hengartner H, Zinkernagel RM. Aplastic anemia rescued by exhaustion of cytokine-secreting CD8 + T cells in persistent infection with lymphocytic choriomeningitis virus. J Exp Med. 1998;187(11):1903–20.
20. Jordan MB, Hildeman D, Kappler J, Marrack P. An animal model of hemophagocytic lymphohistiocytosis (HLH): CD8 + T cells and interferon gamma are essential for the disorder. Blood. 2004;104(3):735–43.
21. Zhou X, Ramachandran S, Mann M, Popkin DL. Role of lymphocytic choriomeningitis virus (LCMV) in understanding viral immunology: past, present and future. Viruses. 2012;4(11):2650–69.
22. Abdel-Hakeem MS. Viruses teaching immunology: role of LCMV model and human viral infections in immunological discoveries. Viruses 2019, 11(2).
23. Barber DL, Wherry EJ, Masopust D, Zhu B, Allison JP, Sharpe AH, Freeman GJ, Ahmed R. Restoring function in exhausted CD8 T cells during chronic viral infection. Nature. 2006;439(7077):682–7.

Publisher's note